

ARTICLE OPEN



Metabolic handoffs between multiple symbionts may benefit the deep-sea bathymodioline mussels

Tal Zvi-Kedem^{1,2}, Simina Vintila³, Manuel Kleiner³, Dan Tchernov² and Maxim Rubin-Blum¹✉

© The Author(s) 2023

Bathymodioline mussels rely on thiotrophic and/or methanotrophic chemosynthetic symbionts for nutrition, yet, secondary heterotrophic symbionts are often present and play an unknown role in the fitness of the organism. The bathymodioline *Idas* mussels that thrive in gas seeps and on sunken wood in the Mediterranean Sea and the Atlantic Ocean, host at least six symbiont lineages that often co-occur. These lineages include the primary symbionts chemosynthetic methane- and sulfur-oxidizing gammaproteobacteria, and the secondary symbionts, Methylophagaceae, Nitrocolaceae and Flavobacteriaceae, whose physiology and metabolism are obscure. Little is known about if and how these symbionts interact or exchange metabolites. Here we curated metagenome-assembled genomes of *Idas modiolaeformis* symbionts and used genome-centered metatranscriptomics and metaproteomics to assess key symbiont functions. The Methylophagaceae symbiont is a methylotrophic autotroph, as it encoded and expressed the ribulose monophosphate and Calvin-Benson-Bassham cycle enzymes, particularly RuBisCO. The Nitrocolaceae ASP10-02a symbiont likely fuels its metabolism with nitrogen-rich macromolecules and may provide the holobiont with vitamin B12. The *Urechidicola* (Flavobacteriaceae) symbionts likely degrade glycans and may remove NO. Our findings indicate that these flexible associations allow for expanding the range of substrates and environmental niches, via new metabolic functions and handoffs.

ISME Communications; <https://doi.org/10.1038/s43705-023-00254-4>

INTRODUCTION

Chemosynthetic symbioses allow animals and some protists to colonize extreme environments including hydrothermal vents and cold seeps in the deep sea, as well as key productive habitats in coastal areas, such as the seagrass meadows [1, 2]. Chemosynthesis, that is, the assimilation of single-carbon molecules, such as carbon dioxide and methane, using the energy stored in reduced compounds, primarily reduced sulfur (sulfide, thiosulfate, elemental sulfur) and methane, fuels these symbioses. Chemosynthetic symbioses are usually characterized by low diversity and high fidelity of key nutritional symbionts at the species level [3]. They exhibit a broad range of transmission strategies, including vertical, horizontal and mixed modes [4], that may determine the fidelity of these associations, as well as the strength of environmental selection for the fittest symbionts and genetic diversity within the symbiont populations [3, 5–7]. As in free-living bacterial populations, genetic diversity broadens the functions of symbionts, allowing the holobiont to acquire new metabolic capabilities and environmental niches [8, 9].

Symbiont taxonomic and functional diversity varies markedly between lineages of bathymodioline mussels, which include the chemosynthetic genera *Bathymodiolus*, *Gigantidas* and *Idas* among others [10]. The key symbionts of bathymodioline mussels include the sulfur-oxidizing Thioglobaceae (gammaproteobacterial order PS1, also known as the SUP05 clade), and the

Methyloprofundus (gammaproteobacterial order Methylococcales) methane-oxidizing bacteria. Some bathymodioline mussels, such as *Bathymodiolus earlougheri*, *B. billschneideri* and *B. nancyschneideri* host single-species populations of thiotrophic symbionts [11], whereas *Gigantidas childressi* and *G. platifrons* host mainly the methane-oxidizing bacteria [12–14]. Others host both [15]. There are also extreme cases of symbiont diversity loss and gain in bathymodioline symbioses. For example, a small deep-sea bathymodioline mussel *Idas argenteus* appears to lack symbionts, which may have been gained in the past and recently lost [16]. Others, such as *B. heckerae*, from the deep Gulf of Mexico, host several taxa of symbionts with distinct functions: apart from two species of methane-oxidizing symbionts and two species of sulfur-oxidizing symbionts, *B. heckerae* has additional bacterial symbionts, including the Methylophagaceae sp. methylotrophs, as well as *Cycloclasticus* that catabolize short-chain alkanes [17–19].

Here we focus on another extreme case of multi-species symbioses in bathymodioline mussels, namely *Idas* mussels from the Mediterranean Sea. Several previous studies noted the co-occurrence of at least six gill symbiont phylotypes in an *Idas* species from the east Atlantic and the Mediterranean Sea; this *Idas* species was first identified as *Idas* sp. MED, and is now called *Idas modiolaeformis* [20–23]. These small mussels thrive in seeps and wood falls and the diversity of their symbionts appears to be linked to the availability and composition of reduced fluids [20].

¹Biology Department, National Institute of Oceanography, Israel Oceanographic and Limnological Research (IOLR), Haifa 3108000, Israel. ²Morris Kahn Marine Research Station, Department of Marine Biology, Leon H. Charney School of Marine Sciences, University of Haifa, Haifa 3498838, Israel. ³Department of Plant and Microbial Biology, North Carolina State University, Raleigh, NC 27695, USA. ✉email: mrubin@ocean.org.il

Received: 18 April 2023 Revised: 25 April 2023 Accepted: 11 May 2023

Published online: 20 May 2023

Early studies identified the following six key phylotypes: the *Methyloprofundus sedimenti*-related type I methanotrophs (M1), two phylotypes of Thioglobaceae sulfur-oxidizing symbionts (S1 and S2), Methylophagaceae methylotrophs (M2), as well as two phylotypes that lacked the potential for being chemosynthetic – Bacteroidetes (CFB) and a gammaproteobacterial lineage (G) [21]. Hereafter we refer to the methanotrophs (M1) and thiotrophs (S1 and S2) as the primary symbionts, and the others as secondary symbionts (M2, CFB, and G). These phylotypes were found to be associated with bacteriocytes in the symbiont-bearing gill tissue using fluorescence *in situ* hybridization (FISH), confirming the symbiotic nature of their association with *I. modiolaeformis* [21, 22]; however, these observations did not provide conclusive evidence for the intracellular localization of all the symbionts [22]. Other variants of the gammaproteobacterial secondary symbionts, were discovered later [20, 23]. While the functions of the primary symbionts and the methylotroph M2 were estimated based on the detection of marker genes, the functionality of the symbiotic methylotrophs has not been studied in detail using omics, and little is known about the role of other symbiont lineages.

We aimed to characterize the metabolism and physiology of the *Idas* symbionts, using genome-centric metagenomics, metatranscriptomics and metaproteomics. We collected 14 *Idas* individuals from hydrocarbon seeps and brine pools off the shore of Israel [24, 25]. We hypothesized that the secondary symbionts may contribute to holobiont fitness by providing important functions via metabolic handoffs. Alternatively, these potential heterotrophs, which are most abundant in mussels that colonize plant debris, such as sunken wood, may extract nutrients from organic substrates [20, 23]. We thus investigated the metabolic potential of the *Idas* symbionts, providing a snapshot of host-symbiont interactions in this specific multi-member symbiosis.

MATERIALS AND METHODS

Sample collection, processing, and sequencing

Hydrocarbon seeps are found at the toe of Palmahim Disturbance, a large deformation feature at the Israeli margin [26, 27] (Supplementary Fig. S1). In 2011 we collected one *Idas* specimen from a carbonate sample that was retrieved, from the Palmahim pockmark 32°09.6'N and 34°10.0'E at a depth of 1036 m, using Hercules remotely operated vehicle (ROV), based on the Nautilus E/V. In 2021, multiple individuals ($n = 14$ studied herein) were collected from the edges of a brine pool at the toe of Palmahim disturbance, at 1,150 m water depth (32° 13.4' N 34° 10.7' E) [25], using the work-class SAAB Seaeye Leopard ROV, based on R/V Bat Galim (Supplementary Fig. S1).

Metagenomics. We preserved a single individual collected in 2011, as well as 5 individuals that were collected in 2021, at -20°C . DNA was extracted from these individuals using the DNeasy Blood & Tissue Kit (Qiagen), following the manufacturer's instructions. DNA libraries were constructed for these six individuals at HyLabs, Israel, and sequenced using 120 million 2×150 bp paired-end reads per sample with an Illumina NovaSeq at GENEWIZ, Germany.

Metatranscriptomics. An additional 4 individuals were preserved in RNAlater. DNA, RNA and proteins were extracted from these individuals using the AllPrep DNA/RNA/Protein Mini Kit (Cat. No. 80004, Qiagen). RNA libraries were constructed for these individuals at Novogene, Singapore, and sequenced using 100 million 2×150 bp paired-end reads per sample with an Illumina NovaSeq, following library construction with the NEBNext Ultra RNA Library Prep Kit for Illumina (Cat No. 7530) and ribosomal RNA depletion with the Ribo-Zero Plus rRNA Depletion Kit (Bacteria) (Cat No. 20037135) & Ribo-Zero Magnetic Kit (Plant Leaf).

Protein extraction and peptide preparation for metaproteomics

We resuspended the protein precipitates from the 4 individuals extracted with the AllPrep DNA/RNA/Protein Mini Kit kit in $60 \mu\text{l}$ of SDT lysis buffer

[4% (w/v) SDS, 100 mM Tris-HCl pH 7.6, 0.1 M DTT] and heated to 95°C for 10 min. The SDT protein mixture was cleaned up, reduced, alkylated and digested using the filter-aided sample preparation (FASP) protocol as described previously [28]. We performed all centrifugation steps mentioned below at $14,000 \times g$. We combined lysates ($60 \mu\text{l}$) with $400 \mu\text{l}$ of urea solution (8 M urea in 0.1 M Tris-HCl pH 8.5) and loaded it onto 10 kDa MWCO $500 \mu\text{l}$ centrifugal filters (VWR International) followed by centrifugation for 20 min. We washed filters once by applying $200 \mu\text{l}$ of urea solution followed by 20 min of centrifugation to remove any remaining SDS. We performed protein alkylation by adding $100 \mu\text{l}$ IAA solution (0.05 M iodoacetamide in urea solution) to each filter and incubating for 20 min at room temperature followed by centrifugation for 20 min. The filters were washed three times with $100 \mu\text{l}$ of urea solution with 15 min centrifugations, followed by a buffer exchange to ABC (50 mM ammonium bicarbonate). Buffer exchange was accomplished by three cycles of adding $100 \mu\text{l}$ of ABC buffer and centrifuging for 15 min. For tryptic digestion, we added $1 \mu\text{g}$ of MS grade trypsin (ThermoFisher Scientific) in $40 \mu\text{l}$ of ABC buffer to each filter and incubated for 16 h in a wet chamber at 37°C . We eluted tryptic peptides by adding $50 \mu\text{l}$ 0.5 M NaCl and centrifuging for 20 min. Peptide concentrations were determined with the Pierce Micro BCA assay (ThermoFisher Scientific) following the manufacturer's instructions.

LC-MS/MS

All proteomic samples were analyzed by 1D-LC-MS/MS as previously described [28]. We loaded $1.2 \mu\text{g}$ of peptide from each sample onto a 5 mm, $300 \mu\text{m}$ ID C18 Acclaim® PepMap100 pre-column (Thermo Fisher Scientific) with an UltiMate™ 3000 RSLCnano Liquid Chromatograph (Thermo Fisher Scientific) in loading solvent A (2% acetonitrile, 0.05% trifluoroacetic acid). Elution and separation of peptides on the analytical column ($75 \text{ cm} \times 75 \mu\text{m}$ EASY-Spray column packed with PepMap RSLC C18, $2 \mu\text{m}$ material, Thermo Fisher Scientific; heated to 60°C) was achieved at a flow rate of 300 ml min^{-1} using a 140 min gradient going from 95% buffer A (0.1% formic acid) and 5% buffer B (0.1% formic acid, 80% acetonitrile) to 31% buffer B in 102 min, then to 50% B in 18 min, and finally to 99% B in 1 min and ending with 99% B. The analytical column was connected to a Q Exactive HF hybrid quadrupole-Orbitrap mass spectrometer (Thermo Fisher Scientific) via an Easy-Spray source. Eluting peptides were ionized via electrospray ionization (ESI). Carryover was reduced by a wash run (injection of $20 \mu\text{l}$ acetonitrile, 99% eluent B) between samples. MS1 spectra were acquired by performing a full MS scan at a resolution of 60,000 on a 380 to 1600 m/z window. MS2 spectra were acquired using data-dependent acquisition, selecting for fragmentation the 15 most abundant peptide ions (Top15) from the precursor MS1 spectra. A normalized collision energy of 25 was applied in the HCD cell to generate the peptide fragments for MS2 spectra. Other settings of the data-dependent acquisition included: a maximum injection time of 100 ms, a dynamic exclusion of 25 s, and the exclusion of ions of +1 charge state from fragmentation. About 50,000 MS/MS spectra were acquired per sample.

Protein identification and quantification

We constructed a protein sequence database for protein identification using the protein sequences predicted from the metagenome-assembled genomes obtained in this study. To identify peptides from the host, we used the annotated protein sequences of the bathymodioline mussel *Bathymodiolus childressi* obtained in a previous study (PRIDE PXD008089-1) [29], since no annotated *Idas* protein sequences were available. We added sequences of common laboratory contaminants by appending the cRAP protein sequence database (<http://www.thegpm.org/crap/>). The final database contained 49,401 protein sequences and is included in the PRIDE submission (see data access statement) in fasta format. Searches of the MS/MS spectra against this database were performed with the Sequest HT node in Proteome Discoverer 2.3.0.523 as previously described [30]. The peptide false discovery rate (FDR) was calculated using the Percolator node in Proteome Discoverer and only peptides identified at a 5% FDR were retained for protein identification. Proteins were inferred from peptide identifications using the Protein-FDR Validator node in Proteome Discoverer with a target FDR of 5%. To estimate species abundances based on proteinaceous biomass using the metaproteomic data we followed the previously-described approach [31] with the added filter criterion of requiring two protein-unique peptides for a protein to be retained for biomass calculations.

Bioinformatics

Metagenomes were assembled using SPAdes V3.15 with $-meta$ $k = 21,33,66,99,127$ parameters [32], following adapter trimming and error correction with *tadpole.sh*, using the BBtools suite following read preparation with the BBtools suite (Bushnell, B, sourceforge.net/projects/bbmap/). Downstream mapping and binning of metagenome-assembled genomes (MAGs) were performed using DASTool, Vamb, Maxbin 2.0 and Metabat2 [33–36] within the Atlas V2.9.1 framework [37], using the genome dereplication nucleotide identity threshold of 0.975. MAG quality was verified using Checkm2 [38] and QUAST [39]. Taxonomy was assigned using GTDB-tk V2.1 [40]. Functional annotation was carried out using the Rapid Annotations using the Subsystems Technology RAST server [41], and key annotations were verified by BLASTing against the NCBI database. RNA reads were quality-trimmed and mapped to the MAGs using BBmap (Bushnell, B, sourceforge.net/projects/bbmap/), and read counts were assigned to coding sequences using FeatureCounts [42]. The counts were normalized as transcripts per million (TPM), separately for each MAG [43].

Phylogenetic analyses were performed with IQ-TREE 2 [44] or MEGA11 [45], based on the best model determined by ModelFinder, following sequence alignment with MAFFT [46]. For phylogenomics, we used GTOtree [47] and Fasttree [48], as implemented in GTOtree. Mitochondrial genomes were assembled with MitoZ [49], rotated with MARS [50] and aligned with MAFFT [46].

Fluorescent in-situ hybridization

Four additional individuals were fixed in 2% paraformaldehyde in 1x phosphate-buffered saline (PBS) for at most 12 h at 4 °C, rinsed three times in 1x PBS, and stored at 4 °C in 0.5x PBS/50% ethanol. Whole tissue from *Idas* individuals was dehydrated, embedded in Steedman's wax, and cut into 8 µm sections as previously described [19]. To identify the secondary symbionts, we used the Cy3-labeled BhecM2-822, ImedaG-193 and CF319 probes, targeting the Methylophagaceae, Nitrospiraceae and Flavobacteriaceae symbionts, respectively [22]. Cy5-labeled EUB338 targeting most bacteria was used as a positive control [51] and the Cy3-labeled NON338 probe was used as a control for background autofluorescence [52]. Photomicrographs were acquired with Nikon A1R Confocal Laser Scanning Microscope, using the Plan Apochromat VC 61.5x objective with oil immersion. The brightness and contrast of the images were adjusted with Adobe Photoshop (Adobe Systems, Inc., USA).

RESULTS AND DISCUSSION

Idas modiolaeformis from the eastern Mediterranean hosts at least six symbiont genotypes

The mussels were identified as *Idas modiolaeformis*, based on the analysis of mitochondrial cytochrome c oxidase I (MT-CO1) sequences from the six metagenomes, using the Barcode of Life Data System identifier. These sequences were 98.4–98.6% similar to those of the *I. modiolaeformis* in the database (for example, the eastern Atlantic individuals, KT216487 in NCBI). The best hits, 98.7–98.9% similarity, were to the sequences of *Idas* individuals recovered from the Nile Deep Sea Fan mud volcano at the depth of 1693 meters (FM212787). Hereafter we refer to our samples as *I. modiolaeformis*, as among other known *Idas* species, the next closest hit was *Idas macdonaldi* with a lower MT-CO1 similarity of 95%. Yet, given that the individuals from the Plamahim Disturbance and the Nile Deep Sea Fan are not genetically identical, it is plausible that genetic exchange between these populations is low. We observed some variation of MT-CO1 and full mitochondrial sequences among the Palmahim individuals corresponding to the occurrence of different haplotypes. Genetic distance may increase with the geographical distance or time, as the individual that we collected in 2011 from a distinct seep located several hundreds of meters from the brine pool site where other individuals were obtained, was the most diverged (Supplementary Fig. S2). Yet, as we discuss below, the host phylotypes were not linked to the symbiont diversity, in agreement with previous findings [20].

We generated metagenome-assembled genomes (MAGs) for the six key *I. modiolaeformis* symbiont phylotypes. We note that besides these six lineages, metagenomic binning resulted in the

discovery of MAGs for two additional taxa – a Rhizobiales alphaproteobacterium, as well as a Bdellovibrionaceae species. Given that the nature of the association between these species and *I. modiolaeformis* is unclear, as they have not been previously described by amplicon sequence, we hereafter focus only on the six previously detected lineages. For these, good or high-quality genomes were assembled and binned (Table 1).

In the previous amplicon-based sequencing studies, the symbionts, particularly the secondary ones, were only classified to class and phylum taxonomic levels. We used our MAGs to obtain improved taxonomic assignments through the Genome Taxonomy Database (GTDB) inference tool and validated their taxonomic placement using phylogenies based on the reference collections of closely related genomes from GenBank. We confirmed that the methane-oxidizing symbionts belonged to the *Methyloprofundus* clade, also known as marine methylotrophic group 1 or MMG1, and verified their placement using a PmoA protein phylogeny, as genomes of most *Methyloprofundus* symbionts are missing from the databases (Supplementary Fig. S3). The sulfur oxidizers belonged to two distinct clades, *Candidatus* Thioglobus A and *Candidatus* Thiodubilierella (GTDB inference, hereafter *Thioglobus* and *Thiodubilierella*). The *Thiodubilierella* genus name has been suggested for the symbionts of *B. septemdiemum* [53], and was integrated into the GTDB taxonomy. Yet, *Thiomultimodus* has been proposed as an alternative name for both the *Thioglobus* and *Thiodubilierella* clades, with two SUP05 A and B subclades [54]. Whereas *Thioglobus* (SUP05 clade A) is often represented by free-living species and clam symbionts, *Thiodubilierella* (SUP05 clade B) has been described only in mussel symbioses [54]. Hereafter we refer only to *Thioglobus* and *Thiodubilierella* nomenclature for the two thiotrophic symbiont clades. The co-occurrence of these clades in an individual has only been documented in *B. heckeriae* [17–19] and *I. modiolaeformis* [22].

The new MAG-based taxonomic assignments greatly improved the classification of the secondary symbionts and allowed us to make predictions about their physiology based on previously characterized relatives. The methylotrophic symbionts were assigned to the Methylophagaceae clade GCA-002733105. Phylogenetic placement based on a tree using single-copy genes indicated that this clade lacks a cultivated representative, and includes lineages commonly found at cold seeps (e.g., the genome of the most closely related lineage, *Methylophaga* GLR1851, was curated from a sample at the Hikurangi Margin gas hydrate deposits), as well as the only other Methylophagaceae symbionts that occur in *B. heckeriae* (Supplementary Fig. S4).

Phylotype G belonged to the Nitrospiraceae family ASP10-02a (Table 1, Supplementary Fig. S5). Nitrospiraceae are rarely found in symbioses; however, the Rs1 and Rs2 symbionts of the bone-eating worm *Osedax* belong to the Nitrospiraceae family (unnamed genus Rs1) [55–57]. Nitrospiraceae are prominent degraders of nitrogen-rich compounds such as amino acids [55, 58, 59], and the ASP10-02a clade is prominent in the water column, often exhibiting high abundance and activity during algal blooms [60, 61]. The symbionts *Idas* and *Osedax* belong to distinct clades within Nitrospiraceae, their 16 S rRNA gene sequences are only ~90% similar and their average nucleotide identity (ANI) is <70%. Given that the hosts thrive on different substrates, and that the symbionts occupy different tissues, we hypothesize that the functionalities of these symbionts may differ.

The Bacteroidota (CFB) phylotype belonged to the genus *Urechidicola* (Flavobacteriaceae) (Table 1, Supplementary Fig. S6). The first cultivated *Urechidicola* genus representative, *U. process*, was isolated from the intestine of a marine spoonworm, *Urechis unicinctus* [62]. Similar to other Flavobacteriaceae, such as the closely related *Lutibacter*, *Urechidicola* can degrade multiple organic compounds, including DNA and starch [62, 63]. The closest relative of the *Urechidicola* symbiont in *Idas* was found in a bone-degrading biofilm, and it is represented by GenBank assembly accession GCA_016744415.1. Taxonomic

Table 1. Taxonomy (GTDB) and completeness (CheckM2) statistics for the *Idas modiolaeformis* symbiont metagenome-assembled genomes.

NCBI BioSample	Class	Order	Family	Genus	Completeness (%)	Contamination (%)	N50 (Mbp)	Size (Mbp)
SAMN33052357	Gammaproteobacteria	Methylococcales	Methylomonadaceae	<i>Methyloprofundus</i>	99.99	0.00	0.030	2.50
SAMN33052358	Gammaproteobacteria	PS1	Thioglobaceae	<i>Thioglobus_A</i>	90.88	0.18	0.010	1.49
SAMN33052359	Gammaproteobacteria	PS1	Thioglobaceae	<i>Thiodubilierella</i>	98.12	0.50	0.014	1.30
SAMN33052360	Gammaproteobacteria	Nitrosococcales	Methylophagaceae	GCA-002733105	99.96	0.34	0.026	2.17
SAMN33052361	Gammaproteobacteria	Pseudomonadales	Nitrincolaceae	ASP10-02a	98.18	0.01	0.037	2.10
SAMN33052362	Bacteroidia	Flavobacteriales	Flavobacteriaceae	<i>Urechidicola</i>	95.79	0.30	0.020	3.36
SAMN33052363	Alphaproteobacteria	Rhizobiales			99.76	0.78	0.034	1.33
NA*	Bdellovibrionia	Bdellovibrionales	Bdellovibrionaceae		73.48	1.76	0.003	1.42

*Not submitted to NCBI due to low completeness.

affiliation suggests that both of these secondary symbionts are likely copiotrophs that can catabolize both difficult-to-degrade and protein-rich organic matter, such as polysaccharides, nucleic acids and peptides, in the marine environment.

The metagenomic read abundances of the primary symbionts varied among the six *Idas* individuals that were analyzed with metagenomics (Fig. 1). A single individual (*Idas* 16) lacked the methane-oxidizing and methylotrophic symbionts. In this individual, the Nitrincolaceae symbiont was the most abundant, and *Urechidicola* was found (metatranscriptomics and metaproteomics were, unfortunately, not performed for this individual). We performed metatranscriptomics and metaproteomics on four individuals, which were distinct from the ones used for metagenomics. In these four individuals, the relative abundances of symbionts were consistent between metatranscriptomics and metaproteomics measurements, showing that the sulfur oxidizers were most abundant in sample 3 (5% and 2% biomass for *Thioglobus* and *Thiodubilierella*, respectively, Fig. 1B, C). It is important to note that the relative abundances obtained from metagenomics cannot be compared directly with the relative abundances obtained with metaproteomics; metagenomics-derived abundances are a good estimator of cell numbers, whereas metaproteomics-derived abundances are a good estimator of species biomass in a microbial population [31]. The methane-oxidizing bacteria were the most abundant in the four samples analyzed with metatranscriptomics (~70–80%) and metaproteomics (~89–98% estimated biomass). The biomasses of the other symbionts were much lower, in the range of 1.6 to 7.2% for both thiotrophs, with only very few peptides detected for *Urechidicola*. In agreement with the previous study [20], our data suggest that the symbiont proportions differ between individuals, likely based on local environmental conditions experienced by individuals. Methylophagaceae symbionts may require methane-oxidizers to be present to supply their substrate methanol. Nitrincolaceae are consistently found among the samples with meta-omics, and are metabolically active, as their genes and proteins were expressed. Methylophagaceae, Nitrincolaceae and *Urechidicola* symbionts appear to co-occur with the primary symbionts in the gill tissue where the primary symbionts were present (Fig. 2), in agreement with previous data [22]. Yet, it is still not clear if the secondary symbionts are extra- or intra-cellular.

Oxidation of methane and its products fuel the *Idas* symbiosis

Methane oxidizers are the key nutritional symbionts of *I. modiolaeformis*, as suggested by their abundance in the metatranscriptomes and metaproteomes. The particulate methane monooxygenase PmoCAB complex was most well-expressed at both mRNA and protein levels (Supplementary Fig. S7, here and hereafter see Supplementary Table S1 for the full list of genes and proteins expressed). The lanthanide-containing XoxF type methanol dehydrogenase was the predominant one; the calcium-dependent enzyme MxaFI was also found but expressed at lower levels. Carbon assimilation and energy conservation from formaldehyde oxidation function via the ribulose monophosphate (RuMP) pathway, using only the Entner–Doudoroff (ED) bypass, but not the Embden–Meyerhof–Parnas (EMP) variant [64], as the *pfk* gene encoding the pyrophosphate-dependent phosphofructokinase was not found in the genomes of the *Methyloprofundus* symbiont of *I. modiolaeformis* (Supplementary Fig. S7). This is similar to *Bathymodiolus japonicus* symbionts and in contrast to those of *Bathymodiolus platifrons*, which have both the ED and EMP variants [65]. The serine cycle is incomplete, as hydroxypyruvate reductase was missing; however, some central proteins of this pathway, such as the serine-glyoxylate aminotransferase and malyl-CoA lyase, were substantially expressed at both the RNA and amino acid levels, indicating that the partial serine pathway is functional (Supplementary Fig. S7) [15]. All the genes in the tricarboxylic acid (TCA, Krebs) cycle were found and expressed,

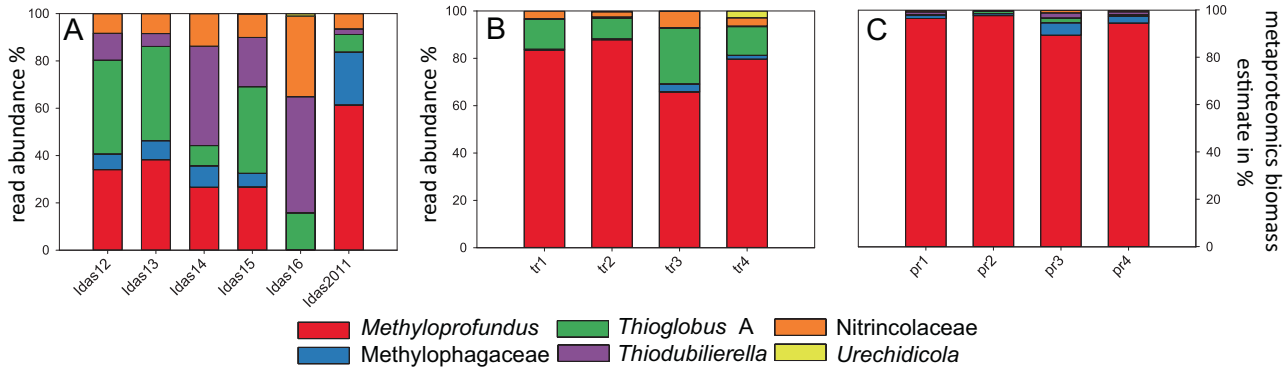


Fig. 1 The relative abundances and biomass distributions of the six key symbiont genotypes in individual *Idas modiolaeformis* specimens. **A** Read abundances in metagenomes (Idas12-16 are samples from the brine pool site, Idas2011 was collected in 2011 from carbonates at a nearby seep site). **B** Read abundances in metatranscriptomes. **C** Biomass estimates based on proteomics following Kleiner et al. 2017. Metatranscriptomics and metaproteomics were performed on the same four individuals (tr1-4 are equivalent to pr1-4). Due to the low confidence of detection, *Urechidicola* proteins were not counted in panel C.

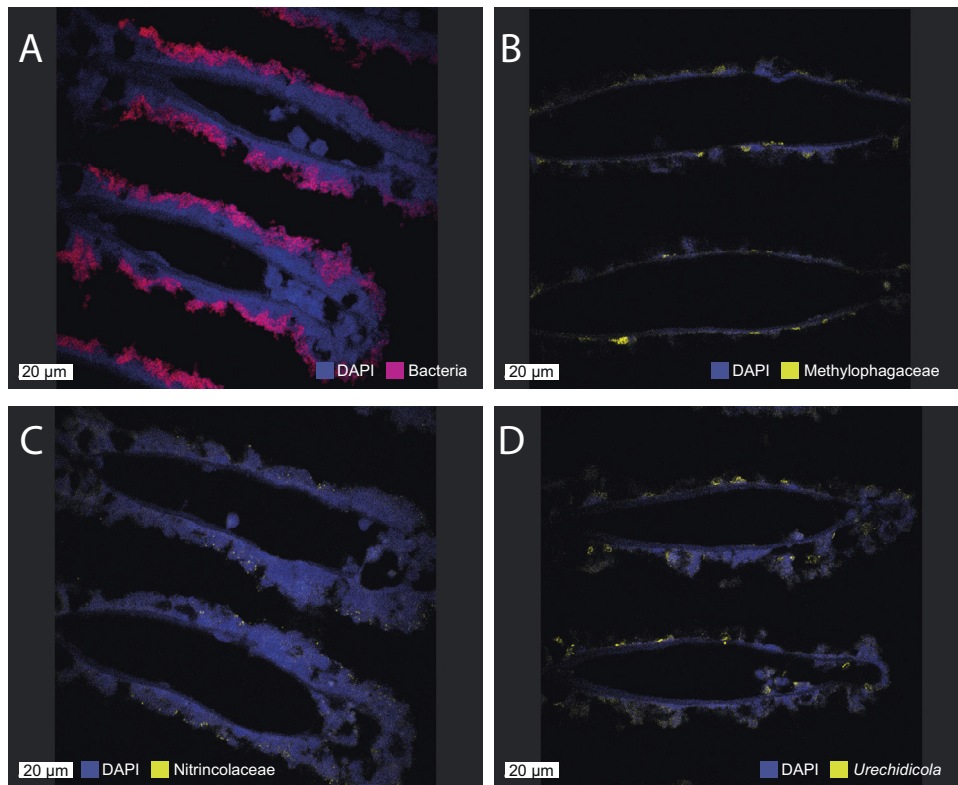


Fig. 2 Fluorescent in situ hybridization (FISH) shows the presence of the secondary symbionts in the *Idas* gill tissue. **A** All the symbiotic bacteria are detected with the EUB338 probe (red), and large methanotroph morphotypes can be observed. **B** Methylophagaceae symbionts (BhecM2-822 probe, yellow) appear to often aggregate along the gill tissue. **C** Nitrincolaceae symbionts (ImedaG-193 probe, yellow) were found sporadically throughout the tissue. **D** Flavobacteriales (*Urechidicola*) symbionts in the gill tissues (CF319, yellow). DAPI staining was used to visualize all DNA. The scale bar is 20 μm .

therefore energy can be conserved through the oxidation of compounds derived from methane assimilation, such as pyruvate (Supplementary Fig. S7). Formaldehyde detoxification and oxidation to CO_2 via the dissimilatory tetrahydromethanopterin route is likely prominent, due to the high expression of this pathway, in particular, that of the 5,6,7,8-tetrahydromethanopterin hydro-lyase (*fae* gene, Supplementary Fig. S7). Both oxygen and nitrate respiration is feasible, given the presence of the respiratory NarGHJ and NirK, yet the respiratory complex IV was expressed at much higher levels, indicating that oxygen is the key electron acceptor for energy conservation (Supplementary Fig. S7).

The metabolism of the Methylophagaceae symbiont is a rare case of methylotrophic autotrophy in chemosynthetic symbioses. Their co-occurrence with the methane oxidizers suggests that they might use methanol, formaldehyde and other metabolites produced by the methane oxidizers. Methane oxidizers excrete metabolites such as methanol, formaldehyde, formate, acetate, and succinate [66–68], which can be used by co-occurring organisms, in particular, methylotrophs [69]. Partnerships between methane oxidizers and methylotrophs are widespread in free-living communities [69, 70], and our results suggest that this association plays a role in *Idas* symbiosis.

lack the 2-oxoglutarate dehydrogenase activity [82–84]. We did not find the 2-oxoglutarate dehydrogenase-encoding genes in the high-quality MAG of the symbiotic *Methylophagaceae*, indicating that the TCA cycle was incomplete. The incomplete TCA allows for the production of intermediates from one-carbon (C1) compounds and prevents futile cycling, that is, the destruction of larger organic compounds via catabolism. This is typical of obligate methylotrophs, such as *Methylobacillus flagellates* [85]. In these bacteria, energy and reducing equivalents may largely result from the oxidation of formaldehyde to CO₂ [85] (Fig. 3).

Variability in terminal electron acceptors, metabolite uptake and vitamin usage may lead to niche differentiation among the thiotrophic symbionts

The two sulfur-oxidizing symbionts, *Thioglobus* and *Thiodubilierella* species, appear to be obligate autotrophs as the key enzymes of the TCA cycle, 2-oxoglutarate dehydrogenase and malate dehydrogenase, were not found in either MAG (Supplementary Fig. S9). This is in agreement with previous observations of symbiotic and free-living organisms from this clade [54, 86, 87]. Both sulfur-oxidizing symbionts have the genes to gain energy from sulfur compounds using the sulfide: quinone oxidoreductase (Sqr), the Sox sulfur oxidation system (SoxYZXAB) and the reverse dissimilatory sulfite reduction (rDSR) system, which catalyzes the oxidation of sulfide to sulfate via the adenosine-5'-phosphosulfate, using the adenylylsulfate reductase and sulfate adenylyltransferase for the two final steps of the pathway. The genes encoding these functions were among the most abundantly transcribed ones in the metatranscriptomes and were often detected at the protein level (Supplementary Fig. S9). Both lineages highly expressed the Calvin-Benson-Bassham cycle enzymes, in particular the two subunits of the type I RuBisCo (in particular, the *rbclS* genes and respective proteins). These obligate autotrophs likely can import some organic compounds similar to the symbionts of *Bathymodiulus azoricus* [15], as TRAP-type dicarboxylate transport systems were encoded and expressed (C4-dicarboxylate and unknown substrate 6 in *Thioglobus*, only the latter in *Thiodubilierella*).

Several differences between *Thioglobus* and *Thiodubilierella* were observed in their terminal electron acceptor use. Only *Thiodubilierella* carried the periplasmic NapABGH for the use of nitrate as a terminal electron acceptor, confirming the modularity of nitrogen metabolism in the *Thioglobaceae* clade [54]. We also found some discrepancies in oxygen respiration were found: *Thioglobus* encoded and highly expressed only the *ccoNOP* genes encoding the *cbb*₃-type cytochrome c oxidase, whereas *Thiodubilierella* encoded three variants (*cbb*₃, *bo*₃, *ba*₃). These terminal oxidases differ in their affinity to O₂ and H₂S [88], likely highlighting adaptation to distinct redox conditions.

Secondary symbionts are heterotrophs that can use nitrogen-rich and difficult-to-degrade metabolites

Data from all three meta-omics approaches suggested that the Nitrospiraceae symbiont is a heterotroph that is capable of using numerous substrates, given the presence and substantial expression of the complete TCA cycle, as well as that of multiple transport systems for organic compounds, such as peptides, amino acids and nucleosides, in line with the metabolic reconstruction of *Osedax* Nitrospiraceae symbionts [55, 59]. Relevant examples include: (1) most enzymes for the degradation of branched-chain amino acids co-occurred in the genomes and were transcribed (Fig. 4); (2) a cluster 11 RfuABCD riboflavin/purine/nucleoside transporter, which clustered with nucleoside degradation enzymes, such as deaminases and phosphorylases (Cda, Ada, DeoABC); (3) the putrescine transport (PotABCD) and degradation system (PuuABCDE) (although the *puuC* gene was not found, likely due to an assembly issue, as these genes occurred at

the edge of a contig). An additional gene cluster encoded the complete PaaA-K and HpaA-I machinery for the catabolism of phenylacetate and hydroxyphenylacetate [89]. This pathway allows for the degradation of recalcitrant, plant-derived organic aromatics, especially in marine bacteria that thrive under fluctuating oxygen conditions in the Mediterranean Sea [90, 91]. Some catabolic reactions may be carried out anaerobically, particularly given the fermentative potential of this bacterium, suggested by the presence of lactate dehydrogenases (some expressed at the mRNA level, Fig. 4). We also identified the genes for nitrate respiration to nitric oxide including the genes for the respiratory nitrate reductase NarGHJ and copper-dependant nitrite reductase NirK. The *nirK* gene was among the most highly expressed genes at the mRNA level in this symbiont (Fig. 4). However, oxygen is likely the key electron acceptor for these symbionts as the *cbb*₃- and *caa*₃ complex IV-encoding genes were highly expressed at the mRNA level (Fig. 4).

A key feature of the metabolism encoded in the *Urechidicola* symbiont genome (Flavobacteriaceae, Bacteroidota) is its potential to degrade glycans (polysaccharides). Bacteroidota, Flavobacteriaceae in particular, are ubiquitous degraders of complex glycans and are found in many environments from human gut mucus to algal blooms in the ocean [92–95]. The diversity of glycans is very large and glycan degradation is carried out by an array of carbohydrate-active enzymes (CAZymes) that are often organized in polysaccharide utilization loci (PULs), which are typical of Bacteroidota [92]. The key features of PULs are the presence of SusCD transporters: the cell surface glycan-binding lipoprotein SusD and the outer membrane TonB-dependent transporter SusC, which can be found in multiple copies in Bacteroidota genomes [96, 97]. We identified four SusCD pairs in the *Urechidicola* symbiont, two of which were among the top 50 most abundantly transcribed genes in the metatranscriptomes, and one SusC protein was detected in the metaproteomes despite the low overall protein identification rate for this symbiont. We note that genomic coding sequence coverage was very low for *Urechidicola* in the metatranscriptome (17%) and metaproteome (5%, mostly with low confidence), and thus only the most active features were detected by these analyses. Given the considerable fragmentation of this genome (300 scaffolds), we couldn't identify large PULs, yet multiple CAZymes were found and often clustered (Fig. 5). For example, a single 30,996 bp contig contained two SusCD pairs, as well as multiple CAZymes, such as DD-carboxypeptidase EC 3.4.16.4; L-Ala-D/L-Glu epimerase EC 5.1.1.20; glucosamine-6-phosphate deaminase EC 3.5.99.6; N-acetylmuramic acid 6-phosphate etherase EC 4.2.1.126; as well as an AmpG family muropeptide MFS transporter; and glycosyl hydrolases of family 18, family 10, and family 3 (Fig. 5). Thus, genomic and transcriptomic data provided evidence for the glycan degrading activity of *Urechidicola*, yet whether the substrates are derived from the gill (e.g., mucus), or the environment remains unknown. To date, FISH analyses do not show clearly if these bacteria are endo- or ectosymbionts of *Idas* gills. One piece of evidence suggesting that they might be ectosymbionts is that cell adhesion appears to play an important role for *Urechidicola*, as a sequence encoding the FAS1 (fascilicin) domain protein was among the top 20 most abundantly transcribed genes [98, 99]. One hypothesis that remains to be explored is whether there are metabolic handoffs between *Urechidicola* and Nitrospiraceae symbionts, for example, via the exchange of aromatic derivatives of polymer degradation, such as phenylacetate and hydroxyphenylacetate [100].

Nitrospiraceae symbionts may contribute to holobiont fitness by producing vitamin B12

The Nitrospiraceae symbiont can produce adenosylcobalamin (vitamin B12), given the presence of almost all the genes needed for its synthesis (Fig. 4), similar to the Nitrospiraceae *Osedax*

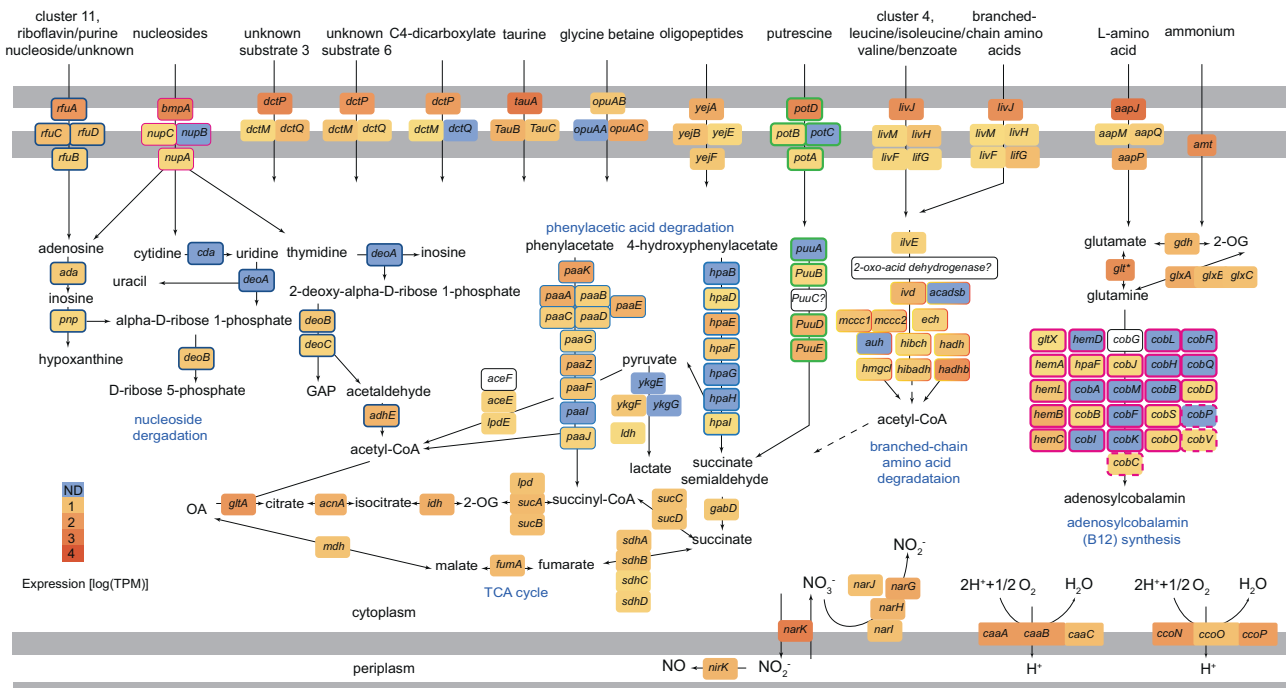


Fig. 4 The Nitricolaceae symbiont can import and catabolize multiple metabolites, including peptides, amino acids (in particular, branched-chain amino acids), nucleosides and some aromatics, such as phenylacetate. The tricarboxylic acid cycle is complete. The symbiont can likely ferment pyruvate to lactate, as the cytochrome c-dependent D-lactate and L-lactate dehydrogenases were found and expressed. A near-complete pathway of adenosylcobalamin (B12) is encoded and partially transcribed. * Among the presented proteins, only the glutamine synthetase (*glt* gene) was expressed at the protein level. Outlines of the same color indicate gene clusters. The following genes are shown: adenosine deaminase *ada*, polyribonucleotide nucleotidyltransferase *pnp*; cytidine deaminase *cda*; thymidine phosphorylase *deoA*; phosphopentomutase *deoB*; deoxyribose-phosphate aldolase *deoC*; aldehyde-alcohol dehydrogenase *adhE*; acetyl-CoA carboxylase *accEF-lpdE*; L-lactate dehydrogenase *ykgEFG*; L-lactate dehydrogenase *ldh*; citrate synthase *gltA*; aconitase *acnA*; isocitrate dehydrogenase *idh*; 2-oxoglutarate dehydrogenase complex *sucAB-lpdE*; succinate-CoA ligase *sucCD*; succinate dehydrogenase *sdhABC*; fumarate hydratase class I, aerobic *fumA*; malate dehydrogenase *mdh*; pyruvate dehydrogenase *aceEF-lpdA*; phenylacetate catabolon *paaA-K*; 4-hydroxyphenylacetate catabolon *hpaB-I*; succinate-semialdehyde dehydrogenase [NADP⁽⁺⁾] *gabD*; putrescine catabolon *puuA-D*; acetolactate synthase *ilvB*; isovaleryl-CoA dehydrogenase *ivd*; short/branched chain specific acyl-CoA dehydrogenase *acadsb*; enoyl-CoA hydratase *ech*; methylcrotonoyl-CoA carboxylase *mcc1,2*; methylglutaconyl-CoA hydratase *auh*; 3-hydroxyisobutyryl-CoA hydrolase *hibch*; hydroxyacyl-coenzyme A dehydrogenase *hadH*; hydroxymethylglutaryl-CoA lyase *hmgcl*; 3-hydroxyisobutyrate dehydrogenase *hibadh*; acetyl-CoA acyltransferase *hadhb*; glutamine synthetase *glt*; glutamate dehydrogenase *gdhA*; glutamine amidotransferase *glxABC*; *cbb*₃-type cytochrome c oxidase *ccoNOP*; *caa*₃-type cytochrome c oxidase *caaABC*; respiratory nitrate reductase *narGHJI*, copper-containing nitrite reductase *nirK*; nitrate/nitrite antiporter *narK*. The putative transporter substrates are mentioned in the figure. Glyceraldehyde 3-phosphate, GAP; oxaloacetate, OA; 2-oxoglutarate, 2-OG. Average expression values from 4 individuals are shown.

symbionts [55, 59]. The *cobG* gene was the only gene, out of 25 genes for vitamin B12 biosynthesis, that was undetected, likely due to the incompleteness of the MAG. Many of the vitamin B12 biosynthesis genes were transcribed and detected in the metatranscriptomes. We also found the genes for vitamin B12 biosynthesis in the methane-oxidizing symbiont, which is a likely key producer of adenosylcobalamin in *I. modiolaeformis*, given its dominant biomass in most individuals (Fig. 1). In hosts that lack the methane-oxidizing symbionts, B12 production by the alternative Nitricolaceae symbionts may be crucial for the holobiont. Nitricolaceae, specifically the ASP10-02a lineage to which the symbionts belong, are (i) dominant species in Earth's cold oceans, (ii) are often associated with algal bloom degradation, (iii) appear to be the most prominent B12 producers in these habitats and (iv) supply B12 specifically to Methylophagaceae, suggesting that B12-based ASP10-02a-methylotroph/autotroph associations can be advantageous under some conditions [61, 101]. The B12-based dynamics play a key role in the water column [102], but also human gut [103] and insect symbioses [104], and thus also may be crucial for chemosynthetic symbioses. The outer membrane receptor BtuB of the vitamin B12 transporter was found in the genomes *Methyloprofundus*, *Thioglobus*, *Urechidicola* and *Methylophagaceae* symbionts. Whereas methane-oxidizing

symbionts are likely prototrophs for cobalamin, but still can take it up from the environment, the other symbionts are auxotrophs and may depend on its uptake.

In bacteria, the key reaction that may depend on cobalamin is methionine synthesis, as cobalamin is required by methionine synthase; thus, the lack of this vitamin may hinder DNA synthesis, methionine regeneration and lead to homocysteine accumulation [105]. *Thiodubilierella* appears to lack the *btuB* gene needed for B12 import; however, unlike the *Thioglobus* symbiont, which encodes only the cobalamin-dependent methionine synthase (MetH; EC 2.1.1.13), *Thiodubilierella* has both the MetH, and the cobalamin-independent methionine synthase (MetE; 5-methyltetrahydropteroyltriglutamate-homocysteine methyltransferase; EC 2.1.1.14), and therefore may not depend on cobalamin for production of the essential amino acid methionine and thus growth [104]. We thus hypothesize, that similar to insect symbioses [104], the interplay between cobalamin requirement, synthesis and uptake may contribute to determining the complexity of *Idas* symbiosis. In our metagenomic dataset, the relative read abundances of Nitricolaceae and *Thiodubilierella*, but not Nitricolaceae and *Thioglobus* symbionts, appear to positively correlate ($R^2 = 0.79$ and $R^2 = 0.03$, respectively, for linear regression of centered-log transformed data). Although

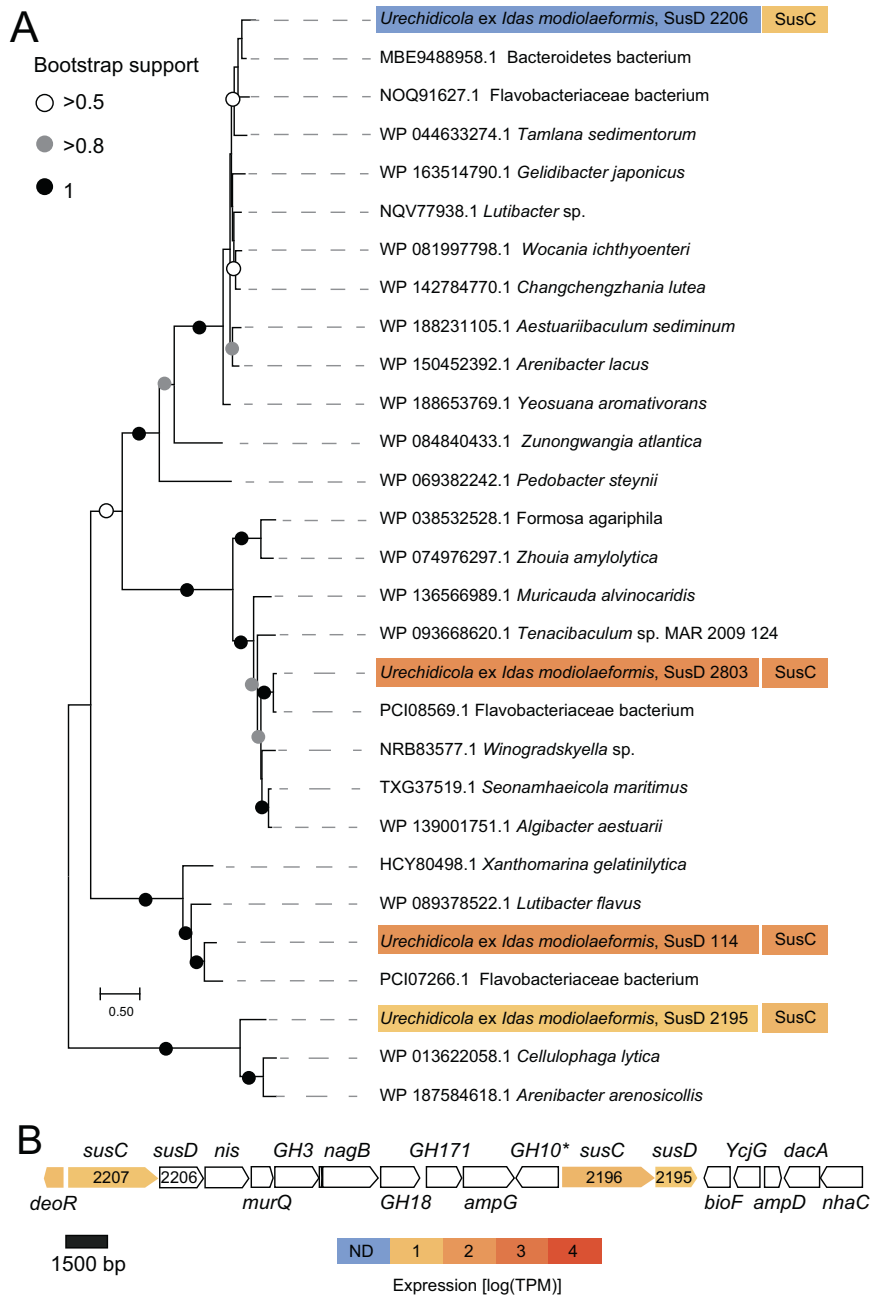


Fig. 5 Polysaccharide utilization loci (PULs) in *Urechidicola* symbionts of *Idas modiolaeformis*. **A** Phylogeny and mRNA-level expression of the SusD proteins (MEGA11, 576 amino acid positions, LG + G + I model). The expression values are based only on a library from a single *Idas* individual, in which expression of these rare symbionts had detectable coverage. **B** The largest contiguous PUL (~27,000 bp) in *Urechidicola* symbiont comprised two *susCD* pairs, as well as genes encoding the following: transcription regulator, *deoR*; sodium/iodide co-transporter, *nis*; N-acetylmuramic acid 6-phosphate etherase, *murQ*; glucosamine-6-phosphate deaminase, *nagB*; MFS permease, *ampG*; aminotransferase, *bioF*; L-Ala-D/L-Glu epimerase, *ycgG*; N-acetylmuramoyl-L-alanine amidase, *ampD*; D-Ala-D-Ala carboxypeptidase, *dacA*; Na⁺/substrate antiporter, *nhaC*; as well as glycoside hydrolases 3, 18, 171, 10. Most of these genes are involved in murein metabolism. * Indicates this gene was identified by an NCBI domain search, but not by dbCAN. The full list of CAZymes is available in Supplementary Table S2. The tree scale represents the number of substitutions per site. Expression values from a single individual (TR4, detectible *Urechidicola* coverage) are shown.

compositional data correlation should be treated with caution, our results hint at the interdependence of these two symbiont populations.

***Urechidicola* symbionts may denitrify to N₂, removing NO**

Urechidicola appears to be the only bacterium capable of complete denitrification to N₂. Nitrate and nitrite reduction can be catalyzed by the periplasmic enzymes heterodimeric nitrate reductase (NapAB, no expression found) and the NrfAB

cytochrome c552 nitrite reductase (both subunits were expressed at the mRNA level). The *norBC* genes that encode the respiratory nitric oxide (NO) reductase were highly transcribed. Most importantly, the *nosZ* gene encoding the periplasmic sec-dependant nitrous oxide reductase was the 11th most abundantly transcribed gene in this bacterium. Both the methane-oxidizing and methylotrophic symbionts can oxidize nitrite to nitric oxide but lack the genes needed to complete the remaining steps of denitrification. Symbiont nitrate respiration can contribute to

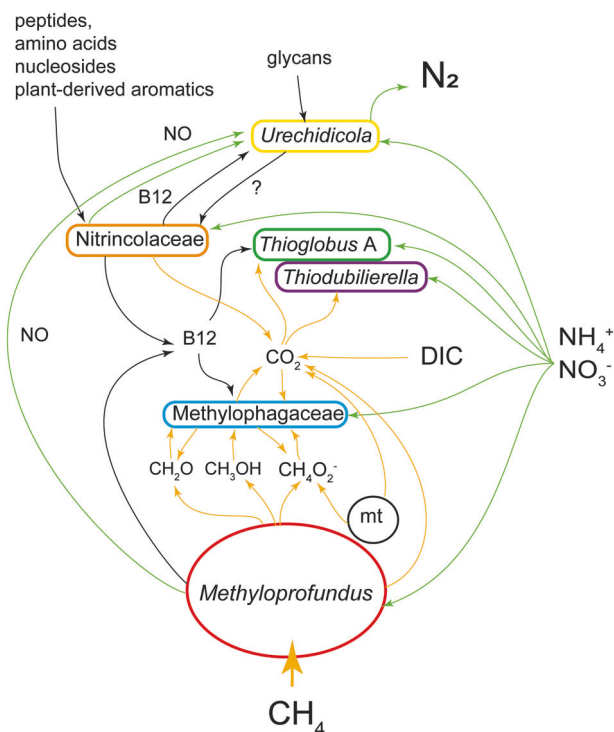


Fig. 6 Schematic representation of hypothetical key metabolic handoffs in the *Idas* symbioses. C1 routes (yellow), nitrogen (green) and macromolecule (black) are highlighted by arrows. For nitrate, the routes comprise both assimilatory and dissimilatory ones. A mitochondrion is included (mt). DIC is dissolved inorganic carbon.

holobiont fitness, as it fuels energy conservation during hypoxia induced by natural perturbations or when the shell valves are closed and reduce competition between host and symbiont for oxygen [15]. Removal of the toxic nitrite respiration product NO could benefit the symbionts [106]. Whereas the *Urechidicola* symbiont is only present in low abundance, complete denitrification is likely beneficial mainly for their population, which can take advantage of excess NO produced by the host or the other symbionts. We speculate that in some cases the *Urechidicola* symbiont may also contribute to NO removal at the holobiont level.

CONCLUSIONS

The *I. modialiformis* symbiosis has a higher number of symbiont species than the typical chemosynthetic associations in most other hosts. The metabolic flexibility in these symbioses expands the range of catabolized substrates and likely allows for the colonization of not only chemosynthetic environments but also organic substrates, such as wood. This nutritional plasticity may have played a role in the adaptation and evolutionary transition of these mussels from organic substrates to the deep sea [107]. Yet, most large bathymodioline mussels, such as *Gigantidas* and most *Bathymodiolus*, host only a few species of chemosynthetic bacteria, highlighting the advantage of limited symbiont diversity. Expanding the symbiont diversity and substrate range may lead to energetic costs, resulting in lower growth rates or reduced reproductive output [20]. These costs may be reduced as only the symbiont that can use the locally abundant substrate grows up to high abundances. For example, at seeps and brine pools, where the key substrate is methane, the methanotrophic symbiont dominates in terms of biomass. We hypothesize that even in the absence of relevant amounts of external organic substrates the secondary symbionts might provide additional

benefits, which include the recycling and efficient use of resources such as NO , methanol and formate, as well as sharing goods such as vitamin B12 (Fig. 6). Some of these positive interactions have equivalents in free-living communities, suggesting that symbiotic interactions may have evolved based on the existing interactions.

DATA AVAILABILITY

DNA and RNA raw reads, as well as symbiont metagenome-assembled genomes, were deposited to NCBI with project accession number PRJNA930646. The mass spectrometry proteomics data have been deposited to the ProteomeXchange Consortium via the PRIDE [108] partner repository with the dataset identifier PXD040273 (Reviewer access at <https://www.ebi.ac.uk/pride/login> with Username: reviewer_pxd040273@ebi.ac.uk and Password: 1Td7u0kv).

REFERENCES

- Dubilier N, Bergin C, Lott C. Symbiotic diversity in marine animals: the art of harnessing chemosynthesis. *Nat Rev Microbiol.* 2008;6:725–40.
- Sogin EM, Kleiner M, Borowski C, Gruber-Vodicka HR, Dubilier N. Life in the dark: phylogenetic and physiological diversity of chemosynthetic symbioses. *Annu Rev Microbiol.* 2021;75:695–718.
- Sato Y, Wippler J, Wentrup C, Ansoerge R, Sadowski M, Gruber-Vodicka H, et al. Fidelity varies in the symbiosis between a gutless marine worm and its microbial consortium. *Microbiome.* 2022;10:178.
- Russell SL. Transmission mode is associated with environment type and taxa across bacteria-eukaryote symbioses: a systematic review and meta-analysis. *FEMS Microbiol Lett.* 2019;366:fnz013.
- Polzin J, Arevalo P, Nussbaumer T, Polz MF, Bright M. Polyclonal symbiont populations in hydrothermal vent tubeworms and the environment. *Proc R Soc B Biol Sci.* 2019;286:20181281.
- Romero Picazo D, Dagan T, Ansoerge R, Petersen JM, Dubilier N, Kupczok A. Horizontally transmitted symbiont populations in deep-sea mussels are genetically isolated. *ISME J.* 2019;13:2954–68.
- Ücker M, Ansoerge R, Sato Y, Sayavedra L, Breusing C, Dubilier N. Deep-sea mussels from a hybrid zone on the Mid-Atlantic Ridge host genetically indistinguishable symbionts. *ISME J.* 2021;15:3076–83.
- Batstone RT, Carscadden KA, Afkhami ME, Frederickson ME. Using niche breadth theory to explain generalization in mutualisms. *Ecology.* 2018;99:1039–50.
- Ansoerge R, Romano S, Sayavedra L, Porras MÁG, Kupczok A, Tegetmeyer HE, et al. Functional diversity enables multiple symbiont strains to coexist in deep-sea mussels. *Nat Microbiol.* 2019;4:2487–97.
- Liu J, Liu H, Zhang H. Phylogeny and evolutionary radiation of the marine mussels (Bivalvia: Mytilidae) based on mitochondrial and nuclear genes. *Mol Phylogenet Evol.* 2018;126:233–40.
- Brzechffa C, Goffredi SK. Contrasting influences on bacterial symbiont specificity by co-occurring deep-sea mussels and tubeworms. *Environ Microbiol Rep.* 2021;13:104–11.
- Wang H, Zhang H, Zhong Z, Sun Y, Wang M, Chen H, et al. Molecular analyses of the gill symbiosis of the bathymodioline mussel *Gigantidas platifrons*. *iScience.* 2021;24:101894.
- Riekenberg PM, Carney RS, Fry B. Trophic plasticity of the methanotrophic mussel *Bathymodiolus childressi* in the Gulf of Mexico. *Mar Ecol Prog Ser.* 2016;547:91–106.
- Wang H, Zhang H, Wang M, Chen H, Lian C, Li C. Comparative transcriptomic analysis illuminates the host-symbiont interactions in the deep-sea mussel *Bathymodiolus platifrons*. *Deep Res Part I Oceanogr Res Pap.* 2019;151:103082.
- Ponnudurai R, Kleiner M, Sayavedra L, Petersen JM, Moche M, Otto A, et al. Metabolic and physiological interdependencies in the *Bathymodiolus azoricus* symbiosis. *ISME J.* 2017;11:463–77.
- Rodrigues CF, Laming SR, Gaudron SM, Oliver G, Le Bris N, Duperron S. A sad tale: Has the small mussel *Idas argenteus* lost its symbionts? *Biol J Linn Soc.* 2015;114:398–405.
- Raggi L, Schubotz F, Hinrichs K-U, Dubilier N, Petersen JM. Bacterial symbionts of *Bathymodiolus* mussels and *Escarpia* tubeworms from Chapopote, an asphalt seep in the Southern Gulf of Mexico. *Environ Microbiol.* 2013;15:1969–87.
- Duperron S, Sibueta M, MacGregor BJ, Kuypers MMM, Fisher CR, Dubilier N. Diversity, relative abundance and metabolic potential of bacterial endosymbionts in three *Bathymodiolus* mussel species from cold seeps in the Gulf of Mexico. *Environ Microbiol.* 2007;9:1423–38.
- Rubin-Blum M, Antony CP, Borowski C, Sayavedra L, Pape T, Sahling H, et al. Short-chain alkanes fuel mussel and sponge *Cycloclasticus* symbionts from deep-sea gas and oil seeps. *Nat Microbiol.* 2017;2:17093.

20. Laming SR, Szafranski KM, Rodrigues CF, Gaudron SM, Cunha MR, Hilário A, et al. Fickle or faithful: The roles of host and environmental context in determining symbiont composition in two bathymodioline mussels. *PLoS One*. 2015;10:e0144307.
21. Laming SR, Duperron S, Cunha MR, Gaudron SM. Settled, symbiotic, then sexually mature: adaptive developmental anatomy in the deep-sea, chemo-symbiotic mussel *Idas modiolaeformis*. *Mar Biol*. 2014;161:1319–33.
22. Duperron S, Halary S, Lorion J, Sibuet M, Gaill F. Unexpected co-occurrence of six bacterial symbionts in the gills of the cold seep mussel *Idas* sp. (Bivalvia: Mytilidae). *Environ Microbiol*. 2008;10:433–45.
23. Rodrigues CF, Cunha MR, Génio L, Duperron S. A complex picture of associations between two host mussels and symbiotic bacteria in the Northeast Atlantic. *Naturwissenschaften*. 2013;100:21–31.
24. Rubin-Blum M, Antler G, Turchyn AV, Tsadok R, Goodman-Tchernov BN, Shemesh E, et al. Hydrocarbon-related microbial processes in the deep sediments of the Eastern Mediterranean Levantine Basin. *FEMS Microbiol Ecol*. 2014;87:780–96.
25. Herut B, Rubin-Blum M, Sisma-Ventura G, Jacobson Y, Bialik OM, Ozer T, et al. Discovery and chemical composition of the eastmost deep-sea anoxic brine pools in the Eastern Mediterranean Sea. *Front Mar Sci*. 2022;9:1040681.
26. Coleman DF, Austin JA, Ben-Avraham Z, Ballard RD. Exploring the Continental Margin of Israel: “Telepresence” at Work. *Eos, Trans Am Geophys Union*. 2011;92:81–82.
27. Gadol O, Tibor G, ten Brink U, Hall JK, Groves-Gidney G, Bar-Am G, et al. Semi-automated bathymetric spectral decomposition delineates the impact of mass wasting on the morphological evolution of the continental slope, offshore Israel. *Basin Res*. 2020;32:1166–93.
28. Wiśniewski JR, Zougman A, Nagaraj N, Mann M. Universal sample preparation method for proteome analysis. *Nat Methods*. 2009;6:359–62.
29. Assié A, Leisch N, Meier DV, Gruber-Vodicka H, Tegetmeyer HE, Meyerdierts A, et al. Horizontal acquisition of a patchwork Calvin cycle by symbiotic and free-living Campylobacterota (formerly Epsilonproteobacteria). *ISME J*. 2020;14:104–22.
30. Mordant A, Kleiner M. Evaluation of sample preservation and storage methods for metaproteomics analysis of intestinal microbiomes. *Microbiol Spectr*. 2021;9:e01877–21.
31. Kleiner M, Thorson E, Sharp CE, Dong X, Liu D, Li C, et al. Assessing species biomass contributions in microbial communities via metaproteomics. *Nat Commun*. 2017;8:1558.
32. Prijbelski A, Antipov D, Meleshko D, Lapidus A, Korobeynikov A. Using SPAdes de novo assembler. *Curr Protoc Bioinforma*. 2020;70:e102.
33. Wu Y-W, Simmons BA, Singer SW. MaxBin 2.0: an automated binning algorithm to recover genomes from multiple metagenomic datasets. *Bioinformatics*. 2015;32:605–7.
34. Sieber CMK, Probst AJ, Sharrar A, Thomas BC, Hess M, Tringe SG, et al. Recovery of genomes from metagenomes via a dereplication, aggregation and scoring strategy. *Nat Microbiol*. 2018;3:836–43.
35. Kang DD, Li F, Kirton E, Thomas A, Egan R, An H, et al. MetaBAT 2: an adaptive binning algorithm for robust and efficient genome reconstruction from metagenome assemblies. *PeerJ*. 2019;2019:e7359.
36. Nissen JN, Johansen J, Allesøe RL, Sønderby CK, Armenteros JJA, Grønbech CH, et al. Improved metagenome binning and assembly using deep variational autoencoders. *Nat Biotechnol*. 2021;39:555–60.
37. Kieser S, Brown J, Zdobnov EM, Trajkovski M, McCue LA. ATLAS: a Snakemake workflow for assembly, annotation, and genomic binning of metagenome sequence data. *BMC Bioinformatics*. 2020;21:257.
38. Chklovskii A, Parks DH, Woodcroft BJ, Tyson GW CheckM2: a rapid, scalable and accurate tool for assessing microbial genome quality using machine learning. *bioRxiv* 2022; 2022.07.11.499243v1.
39. Gurevich A, Saveliev V, Vyahhi N, Tesler G. QUAST: quality assessment tool for genome assemblies. *Bioinformatics*. 2013;29:1072–5.
40. Chaumeil PA, Mussig AJ, Hugenholtz P, Parks DH. GTDB-Tk v2: memory friendly classification with the genome taxonomy database. *Bioinformatics*. 2022;38:5315–6.
41. Aziz RK, Bartels D, Best AA, DeJongh M, Disz T, Edwards RA, et al. The RAST server: rapid annotations using subsystems technology. *BMC Genomics*. 2008;9:75.
42. Liao Y, Smyth GK, Shi W. FeatureCounts: an efficient general purpose program for assigning sequence reads to genomic features. *Bioinformatics*. 2014;30:923–30.
43. Wagner GP, Kin K, Lynch VJ. Measurement of mRNA abundance using RNA-seq data: RPKM measure is inconsistent among samples. *Theory Biosci*. 2012;131:281–5.
44. Minh BQ, Schmidt HA, Chernomor O, Schrempf D, Woodhams MD, Von Haeseler A, et al. IQ-TREE 2: New models and efficient methods for phylogenetic inference in the genomic era. *Mol Biol Evol*. 2020;37:1530–4.
45. Tamura K, Stecher G, Kumar S. MEGA11: molecular evolutionary genetics analysis Version 11. *Mol Biol Evol*. 2021;38:3022–7.
46. Katoh K, Standley DM. MAFFT multiple sequence alignment software version 7: Improvements in performance and usability. *Mol Biol Evol*. 2013;30:772–80.
47. Lee MD, Ponty Y. GTOTree: a user-friendly workflow for phylogenomics. *Bioinformatics*. 2019;35:4162–4.
48. Price MN, Dehal PS, Arkin AP. Fasttree: computing large minimum evolution trees with profiles instead of a distance matrix. *Mol Biol Evol*. 2009;26:1641–50.
49. Meng G, Li Y, Yang C, Liu S. MitoZ: a toolkit for animal mitochondrial genome assembly, annotation and visualization. *Nucleic Acids Res*. 2019;47:e63.
50. Ayad LAK, Pissis SP. MARS: improving multiple circular sequence alignment using refined sequences. *BMC Genomics*. 2017;18:86.
51. Amann RL, Binder BJ, Olson RJ, Chisholm SW, Devereux R, Stahl DA. Combination of 16S rRNA-targeted oligonucleotide probes with flow cytometry for analyzing mixed microbial populations. *Appl Environ Microbiol*. 1990;56:1919–25.
52. Wallner G, Amann R, Beisker W. Optimizing fluorescent in situ hybridization with rRNA-targeted oligonucleotide probes for flow cytometric identification of microorganisms. *Cytometry*. 1993;14:136–43.
53. Russell SL, Pepper-Tunick E, Svedberg J, Byrne A, Ruelas Castillo J, Vollmers C, et al. Horizontal transmission and recombination maintain forever young bacterial symbiont genomes. *PLOS Genet*. 2020;16:e1008935.
54. Ansoorge R, Romano S, Sayavedra L, Rubin-Blum M, Gruber-Vodicka H, Scilipoti S, et al. The hidden pangenome: comparative genomics reveals pervasive diversity in symbiotic and free-living sulfur-oxidizing bacteria. *bioRxiv*. 2020.12.11.421487; <https://doi.org/10.1101/2020.12.11.421487>.
55. Goffredi SK, Yi H, Zhang Q, Klann JE, Struve IA, Vrijenhoek RC. Genomic versatility and functional variation between two dominant heterotrophic symbionts of deep-sea *Osedax* worms. *ISME J*. 2014;8:908–24.
56. Salathé RM, Vrijenhoek RC. Temporal variation and lack of host specificity among bacterial endosymbionts of *Osedax* bone worms (Polychaeta: Siboglinidae). *BMC Evol Biol*. 2012;12:189.
57. Hewitt OH, Diez C, Sergi V. Microbial insights from Antarctic and Mediterranean shallow - water bone - eating worms. *Polar Biol*. 2020;43:1605–21.
58. Lian J, Zheng X, Zhuo X, Chen YL, He C, Zheng Q, et al. Microbial transformation of distinct exogenous substrates into analogous composition of recalcitrant dissolved organic matter. *Environ Microbiol*. 2021;23:2389–403.
59. Martín-Durán J, Moggioli G, Panossian B, Sun Y, Thiel D, Martín-Zamora F, et al. Distinct genomic routes underlie transitions to specialised symbiotic lifestyles in deep sea annelid worms. *Res Sq*. 2022; rs-2049397.
60. Munson-McGee JH, Lindsay MR, Sintes E, Brown JM, D’Angelo T, Brown J, et al. Decoupling of respiration rates and abundance in marine prokaryoplankton. *Nature*. 2022;612:764–70.
61. Bertrand EM, McCrow JP, Moustafa A, Zheng H, McQuaid JB, Delmont TO, et al. Phytoplankton-bacterial interactions mediate micronutrient colimitation at the coastal Antarctic sea ice edge. *Proc Natl Acad Sci USA*. 2015;112:9938–43.
62. Shin SK, Yi H. *Urechidicola croceus* gen. nov., sp. nov., a member of the family Flavobacteriaceae. *Int J Syst Evol Microbiol*. 2020;70:1751–7.
63. Wasmund K, Pelikan C, Schintlmeister A, Wagner M, Watzka M, Richter A, et al. Genomic insights into diverse bacterial taxa that degrade extracellular DNA in marine sediments. *Nat Microbiol*. 2021;6:885–98.
64. Kalyuzhnaia MG, Yang S, Rozova ON, Smalley NE, Clubb J, Lamb A, et al. Highly efficient methane biocatalysis revealed in a methanotrophic bacterium. *Nat Commun*. 2013;4:2785.
65. Hirayama H, Takaki Y, Abe M, Imachi H, Ikuta T, Miyazaki J, et al. Multispecies populations of methanotrophic *Methyloprofundus* and cultivation of a likely dominant species from the Iheya North deep-sea hydrothermal field. *Appl Environ Microbiol*. 2022;88:e0075821.
66. Meulepas RJW, Jagersma CG, Khadem AF, Stams AJM, Lens PNL. Effect of methanogenic substrates on anaerobic oxidation of methane and sulfate reduction by an anaerobic methanotrophic enrichment. *Appl Microbiol Biotechnol*. 2010;87:1499–506.
67. Xin J, Zhang Y, Zhang S, Xia C, Li S. Methanol production from CO₂ by resting cells of the methanotrophic bacterium *Methylosinus trichosporium* IMV 3011. *J Basic Microbiol*. 2007;47:426–35.
68. Gilman A, Fu Y, Hendershott M, Chu F, Puri AW, Smith AL, et al. Oxygen-limited metabolism in the methanotroph *Methylobacterium buryatense* 5GB1C. *PeerJ*. 2017;5:e3945.
69. van Grinsven S, Sinnighe Damsté JS, Harrison J, Villanueva L. Impact of electron acceptor availability on methane-influenced microorganisms in an enrichment culture obtained from a stratified lake. *Front Microbiol*. 2020;11:715.
70. van Grinsven S, Sinnighe Damsté JS, Harrison J, Polerecky L, Villanueva L. Nitrate promotes the transfer of methane-derived carbon from the methanotroph *Methylobacter* sp. to the methylotroph *Methylothermus* sp. in eutrophic lake water. *Limnol Oceanogr*. 2021;66:878–91.
71. Jormakka M, Byrne B, Iwata S. Formate dehydrogenase - A versatile enzyme in changing environments. *Curr Opin Struct Biol*. 2003;13:418–23.

72. Iwadate Y, Funabasama N, Kato JI. Involvement of formate dehydrogenases in stationary phase oxidative stress tolerance in *Escherichia coli*. *FEMS Microbiol Lett.* 2017;364:1–8.
73. Abaibou H, Pommier J, Benoit S, Giordano G, Mandrand-Berthelot MA, Benoit P, et al. Expression and characterization of the *Escherichia coli fdo* locus and a possible physiological role for aerobic formate dehydrogenase. *J Bacteriol.* 1995;177:7141–9.
74. Sawers G, Heider J, Zehelein E, Bock A. Expression and operon structure of the *sel* genes of *Escherichia coli* and identification of a third selenium-containing formate dehydrogenase isoenzyme. *J Bacteriol.* 1991;173:4983–93.
75. Pietzke M, Meiser J, Vazquez A. Formate metabolism in health and disease. *Mol Metab.* 2020;33:23–37.
76. Robinson JJ, Scott KM, Swanson ST, O'Leary MH, Horken K, Tabita FR, et al. Kinetic isotope effect and characterization of form II RubisCO from the chemoautotrophic endosymbionts of the hydrothermal vent tubeworm *Riftia pachyptila*. *Limnol Oceanogr.* 2003;48:48–54.
77. Horken KM, Tabita FR. Closely related form I ribulose biphosphate carboxylase/oxygenase molecules that possess different CO₂/O₂ substrate specificities. *Arch Biochem Biophys.* 1999;361:183–94.
78. Berg IA. Ecological aspects of the distribution of different autotrophic CO₂ fixation pathways. *Appl Environ Microbiol.* 2011;77:1925–36.
79. Zheng P, Wang M, Li C, Sun X, Wang X, Sun Y, et al. Insights into deep-sea adaptations and host–symbiont interactions: A comparative transcriptome study on *Bathymodiolus* mussels and their coastal relatives. *Mol Ecol.* 2017;26:5133–48.
80. Quasem I, Achille AN, Caddick BA, Carter TA, Daniels C, Delaney JA, et al. Peculiar citric acid cycle of hydrothermal vent chemolithoautotroph *Hydrogenovibrio crunogenus*, and insights into carbon metabolism by obligate autotrophs. *FEMS Microbiol Lett.* 2017;364:fnx148.
81. Wood AP, Aurikko JP, Kelly DP. A challenge for 21st century molecular biology and biochemistry: What are the causes of obligate autotrophy and methanotrophy? *FEMS Microbiol Rev.* 2004;28:335–52.
82. Antony CP, Doronina NV, Boden R, Trotsenko YA, Shouche YS, Colin Murrell J. *Methylophaga lonarensis* sp. nov., a moderately haloalkaliphilic methylotroph isolated from the soda lake sediments of a meteorite impact crater. *Int J Syst Evol Microbiol.* 2012;62:1613–8.
83. Shmareva MN, Doronina NV, Tarlachkov SV, Vasilenko OV, Trotsenko YA. *Methylophagamaralis* Bur 1, a haloalkaliphilic methylotroph isolated from the Khliganta soda lake (Southern Transbaikalia, Buryat Republic). *Microbiol (Russian Fed).* 2018;87:33–46.
84. Kim HG, Doronina NV, Trotsenko YA, Kim SW. *Methylophaga aminisulfidivonae* sp. nov., a restricted facultatively methylotrophic marine bacterium. *Int J Syst Evol Microbiol.* 2007;57:2096–101.
85. Chistoserdova L, Lapidus A, Han C, Goodwin L, Saunders L, Brettin T, et al. Genome of *Methylobacillus flagellatus*, molecular basis for obligate methylotrophy, and polyphyletic origin of methylotrophy. *J Bacteriol.* 2007;189:4020–7.
86. Perez M, Breusing C, Angers B, Beinart RA, Won Y-J, Young CR. Divergent paths in the evolutionary history of maternally transmitted clam symbionts. *Proc R Soc B Biol Sci.* 2022;289:20212137.
87. Dede B, Hansen CT, Neuholz R, Schnetger B, Kleint C, Walker S, et al. Niche differentiation of sulfur-oxidizing bacteria (SUP05) in submarine hydrothermal plumes. *ISME J.* 2022;16:1479–90.
88. Schmitz RA, Peeters SH, Versantvoort W, Picone N, Pol A, Jetten MSM, et al. Verrucomicrobial methanotrophs: Ecophysiology of metabolically versatile acidophiles. *FEMS Microbiol Rev.* 2021;45:fuab007.
89. Luengo JM, García JL, Olivera ER. The phenylacetyl-CoA catabolon: a complex catabolic unit with broad biotechnological applications. *Mol Microbiol.* 2001;39:1434–42.
90. Bugg TDH, Ahmad M, Hardiman EM, Rahmanpour R. Pathways for degradation of lignin in bacteria and fungi. *Nat Prod Rep.* 2011;28:1883.
91. Woo HL, Hazen TC. Enrichment of bacteria from Eastern Mediterranean sea involved in lignin degradation via the phenylacetyl-CoA pathway. *Front Microbiol.* 2018;9:922.
92. Martens EC, Koropatkin NM, Smith TJ, Gordon JI. Complex glycan catabolism by the human gut microbiota: The Bacteroidetes sus-like paradigm. *J Biol Chem.* 2009;284:24673–7.
93. Ndeh D, Gilbert HJ. Biochemistry of complex glycan depolymerisation by the human gut microbiota. *FEMS Microbiol Rev.* 2018;42:146–64.
94. Martens EC, Chiang HC, Gordon JI. Mucosal glycan foraging enhances fitness and transmission of a saccharolytic human gut bacterial symbiont. *Cell Host Microbe.* 2008;4:447–57.
95. Fernández-Gómez B, Richter M, Schüler M, Pinhasi J, Acinas SG, González JM, et al. Ecology of marine bacteroidetes: A comparative genomics approach. *ISME J.* 2013;7:1026–37.
96. Reeves AR, D'Elia JN, Frias J, Salyers AA. A Bacteroides thetaiotaomicron outer membrane protein that is essential for utilization of maltooligosaccharides and starch. *J Bacteriol.* 1996;178:823–30.
97. Grondin JM, Tamura K, Déjean G, Abbott DW, Brumer H. Polysaccharide utilization loci: Fueling microbial communities. *J Bacteriol.* 2017;199.
98. Williams TJ, Wilkins D, Long E, Evans F, Demaere MZ, Raftery MJ, et al. The role of planktonic Flavobacteria in processing algal organic matter in coastal East Antarctica revealed using metagenomics and metaproteomics. *Environ Microbiol.* 2013;15:1302–17.
99. Moody RG, Williamson MP. Structure and function of a bacterial Fasciclin I Domain Protein elucidates function of related cell adhesion proteins such as TGFβ1p and periostin. *FEBS Open Bio.* 2013;3:71–77.
100. Liu D, Yan X, Si M, Deng X, Min X, Shi Y, et al. Bioconversion of lignin into bioplastics by *Pandoraea* sp. B-6: molecular mechanism. 2019;26:2761–70.
101. Delmont TO, Murat Eren A, Vineis JH, Post AF. Genome reconstructions indicate the partitioning of ecological functions inside a phytoplankton bloom in the Amundsen Sea, Antarctica. *Front Microbiol.* 2015;6:1–19.
102. Sañudo-Wilhelmy SA, Gobler CJ, Okbami Michael M, Taylor GT. Regulation of phytoplankton dynamics by vitamin B12. *Geophys Res Lett.* 2006;33:10–13.
103. Degnan PH, Taga ME, Goodman AL. Vitamin B12 as a modulator of gut microbial ecology. *Cell Metab.* 2014;20:769–78.
104. McCutcheon JP, McDonald BR, Moran NA. Convergent evolution of metabolic roles in bacterial co-symbionts of insects. *Proc Natl Acad Sci USA.* 2009;106:15394–9.
105. Roth JR, Lawrence JG, Bobik TA. Cobalamin (coenzyme B12): synthesis and biological significance. *Annu Rev Microbiol.* 1996;50:137–81.
106. Porrini C, Ramarao N, Tran SL. Dr. NO and Mr. Toxic - The versatile role of nitric oxide. *Biol Chem.* 2020;401:547–72.
107. Miyazaki JI, de Oliveira Martins L, Fujita Y, Matsumoto H, Fujiwara Y. Evolutionary process of deep-sea *Bathymodiolus* mussels. *PLoS One.* 2010;5:e10363.
108. Perez-Riverol Y, Bai J, Bandla C, García-Seisdedos D, Hewapathirana S, Kamatchinathan S, et al. The PRIDE database resources in 2022: a hub for mass spectrometry-based proteomics evidences. *Nucleic Acids Res.* 2022;50:D543–D552.

ACKNOWLEDGEMENTS

We thank all individuals who helped during the expeditions, including onboard technical and scientific personnel, the captains and crew of the R/V Bat Galim and E/V Nautilus, and teams operating ROVs “Hercules” and “Yona”. This research used samples and data provided by the E/V Nautilus Exploration Program—expedition NA019. We thank Sharon Tal at the Histology Service Unit at the University of Haifa and Boris Shklyar at the Bioimaging unit, Faculty of the Natural Sciences, University of Haifa. We are grateful to Dr. Heather Maughan for editing and feedback on the manuscript. This study was funded by the Israeli Science Foundation (ISF, grant 913/19 to MR-B), the U.S.-Israel Binational Science Foundation (BSF, grant no. 2019055 to MR-B and MK), the Israel Ministry of Energy (grant no. 221-17-002 to MR-B) and the US National Science Foundation (grant IOS 2003107 to MK).

AUTHOR CONTRIBUTIONS

TZ-K, MR-B and DT conceived this study. TZ-K conducted microscopy. MR-B performed bioinformatics. SV and MK performed proteomics. MR-B and TZ-K compiled the data. MR-B, DT and MK acquired funding. TZ-K, MR-B and MK wrote the paper with the contributions of all co-authors.

COMPETING INTERESTS

The authors declare no competing interests.

ADDITIONAL INFORMATION

Supplementary information The online version contains supplementary material available at <https://doi.org/10.1038/s43705-023-00254-4>.

Correspondence and requests for materials should be addressed to Maxim Rubin-Blum.

Reprints and permission information is available at <http://www.nature.com/reprints>

Publisher's note Springer Nature remains neutral with regard to jurisdictional claims in published maps and institutional affiliations.



Open Access This article is licensed under a Creative Commons Attribution 4.0 International License, which permits use, sharing, adaptation, distribution and reproduction in any medium or format, as long as you give appropriate credit to the original author(s) and the source, provide a link to the Creative Commons license, and indicate if changes were made. The images or other third party material in this article are included in the article's Creative Commons license, unless indicated otherwise in a credit line to the material. If material is not included in the article's Creative Commons license and your intended use is not permitted by statutory regulation or exceeds the permitted use, you will need to obtain permission directly from the copyright holder. To view a copy of this license, visit <http://creativecommons.org/licenses/by/4.0/>.

© The Author(s) 2023